

Ordering and interactions between Cl adatoms on Cu(111) and their influence on the local electronic properties as measured by STM and STS

Samuel Torsney, Borislav Naydenov, and John J. Boland*

School of Chemistry, Centre for Research on Adaptive Nanostructures and Nanodevices (CRANN) and Advanced Materials and Bioengineering Research (AMBER) Center, Trinity College Dublin, Dublin 2, Ireland

(Received 26 September 2017; revised manuscript received 24 November 2017; published 14 December 2017)

We present a scanning tunneling microscopy/spectroscopy study of compressed Cl adlayers on Cu(111) under ultrahigh-vacuum conditions. We describe a rational scheme to assign Cl adatoms to different surface sites. The dominant electronic state visible in scanning tunneling spectroscopy (STS) corresponds to an antibonding interaction between the Cl adlayer and the copper surface. This state was observed to be 200 meV higher in energy at hcp sites compared to fcc sites, and it is attributed to the greater charge transfer to Cl adatoms at hcp sites. Although there was no STS signature associated with bridging sites, the presence of bridging Cl adatoms along the periphery of fcc domains caused a shift in the energy of the interface state in the latter. These results shed important light on the ordering and interaction between Cl adatoms on Cu(111) and their influence of the local electronic structure of the surface.

DOI: [10.1103/PhysRevB.96.245411](https://doi.org/10.1103/PhysRevB.96.245411)

I. INTRODUCTION

The interplay between adsorbate-substrate and adsorbate-adsorbate interactions is one of the most extensively studied aspects of surface science. Much of the early work investigated the dependence of the adsorption energy on coverage, and typically showed a decrease in binding energy at higher coverage, ostensibly due to steric repulsions between adsorbates. The simplest systems to study are monatomic adsorbates such as hydrogen or halogens where repulsions are not complicated by the internal structure and the relaxation dynamics of the molecule. In this work, we investigate the packing and the evolution of the electronic structure of Cu(111) under different Cl atom coverage conditions.

The structure of chlorine adsorbed on Cu(111) has already been studied extensively. The initial studies used low-energy electron diffraction (LEED) [1], but more recently these have been followed by photoelectron diffraction [2], surface-extended x-ray absorption fine structure (SEXAFS) [3], and x-ray standing-wave techniques [4,5]. The introduction of scanning tunneling microscopy (STM) [6] has allowed investigation of local features, with atomic resolution, which are averaged out by other techniques. Most of the published research has been focused on the structure and desorption behavior of the chlorine adlayer [7], with the electronic properties of the Cl-Cu(111) surface being less well studied. Some first-principles calculations have been performed, including a detailed paper by Peljhan and Kokalj, which describes the electronic properties of the surface at various Cl coverages [8]. Almost all existing studies focus on surfaces that are formed *via* dissociation of molecular chlorine in vacuum. Jones and Clifford reported that chloroform adsorbs dissociatively on Cu(111), saturating at the $(\sqrt{3} \times \sqrt{3})R30^\circ$ structure [9]. Here we find that the surface coverage does not saturate at 1/3 ML when electrospray deposition is used.

Figure 1 shows the various adsorption sites on a fcc(111) surface. In this figure and throughout the paper, adatoms in fcc,

hcp, and bridge sites are colored black, pink, and green, respectively. As Cl atoms are added to the Cu(111) surface they form chains, where the adjacent atoms alternate between adsorption in fcc and hcp sites, or small $(\sqrt{3} \times \sqrt{3})R30^\circ$ islands with the Cl atoms in fcc sites [10]. As the coverage increases, a porous structure is formed with voids enclosed by the aforementioned Cl chains or $(\sqrt{3} \times \sqrt{3})R30^\circ$ ribbons. The voids close as more Cl atoms are added to the surface until the coverage reaches 1/3 ML, where a uniform $(\sqrt{3} \times \sqrt{3})R30^\circ$ adlayer is formed [1]. Above 1/3 ML, Cl atoms form crowdion interstitials where some of the Cl atoms surrounding the interstitial are displaced from fcc sites to hcp or bridge sites [11]. These crowdion interstitials condense into domain walls as the number density increases [12]. A section of a domain wall is shown in Fig. 1, where the Cl atoms transition from a $(\sqrt{3} \times \sqrt{3})R30^\circ$ domain in which the Cl atoms occupy fcc sites to one in which they occupy hcp sites by passing through a line of atoms in bridge sites. The size of these domains shrinks with increasing Cl coverage until at 0.4 ML the fcc and hcp domains are each one atomic row wide [11]. Between 0.4 and 5/12 ML, the mesh is further compressed such that some of the Cl atomic rows are in sites intermediate between bridge and hollow. Above 5/12 ML, further uniaxial compression of the surface mesh is unfavorable because it would result in Cl-Cl nearest-neighbor distances smaller than the Van der Waals diameter of chlorine [13].

The tradeoff between steric and electronic energy in minimizing the free energy gives rise to this variety of complex structures. This makes the Cl-Cu(111) system ideal for studying the chemical potential by analyzing the surface structure and electronic properties as a function of coverage.

Here, the electronic properties of uniaxially compressed Cl-Cu(111) are studied using resolution scanning tunneling microscopy (STM) and spectroscopy (STS). We begin by analyzing the topography of uniaxially compressed Cl-Cu(111) surfaces, and we deduce the adsorption site of the atoms in the structure. We then use these observations to derive a more general relationship between the coverage and the observed structure in the uniaxial compression regime. STS of the Cl-Cu(111) surface is presented and found to depend on the

*Corresponding author: jboland@tcd.ie

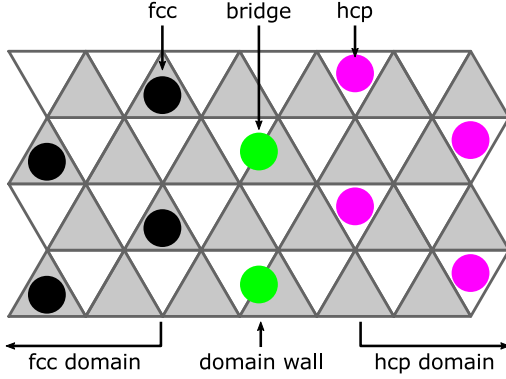


FIG. 1. The different adsorption sites on an fcc(111) surface. The vertices of the triangular grid represent surface atoms, with the shaded triangles representing fcc sites and the empty triangles representing hcp sites. The black, pink, and green circles represent adatoms in fcc, hcp, and bridge sites, respectively. This color scheme is used throughout this paper.

registry of the domain on which it is measured, i.e., whether the constituent atoms occupy fcc or hcp sites. The electronic structure was also found to depend on the size of the domain, and an explanation of this dependence is proposed.

II. EXPERIMENT

All experiments were performed at 77 K using a CreaTec cryogenic STM. The ultrahigh-vacuum (UHV) system includes analysis, preparation, and load-lock chambers with base pressures $<1 \times 10^{-11}$, 2×10^{-11} , and 6×10^{-11} mbar, respectively. The Cu(111) sample was prepared by multiple cycles of Ar^+ bombardment followed by annealing up to 800 K. The chlorine adlayer was formed by electro spraying HPLC grade chloroform onto the Cu(111) surface in vacuum, whereon it is known to dissociate [9]. The electro spray apparatus is commercially available (MolecularSpray) and produces an electro spray jet in ambient that then enters the vacuum system through differentially pumped stages. During deposition, the pressure in the load-lock rises to 1×10^{-6} mbar. However, this is measured far from the sample, and, as a result, the pressure at the sample is expected to be at least an order of magnitude higher. The pressure recovers to 1×10^{-8} mbar seconds after the electro spray gate is closed, and returns to base pressure within 1 h. Tungsten probes were annealed *in situ* and inked on Pt(111) as described previously [14] in order to ensure there were no features in the tip local density of states (LDOS) in the bias range of interest.

III. RESULTS AND DISCUSSION

Electro spray deposition of chloroform onto Cu(111) results in a Cl adlayer with coverage between 3/8 and 7/19 ML. The reaction of chloroform with Cu(111) was previously reported to self-terminate at the $(\sqrt{3} \times \sqrt{3})R30^\circ$ structure (1/3 ML) [9]. We attribute the higher coverage obtained here to the action of the electro spray. During exposure of the sample to the well-collimated electro sprayed molecular beam, there is high pressure at the sample and the adsorbed Cl atoms may

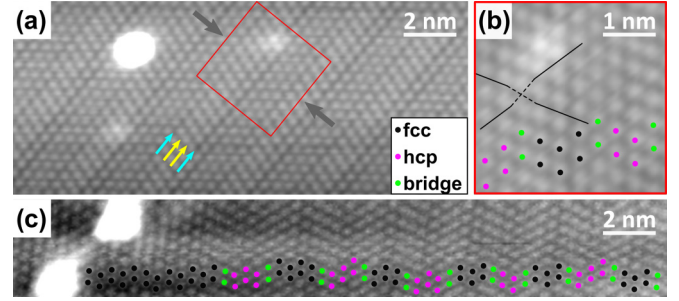


FIG. 2. Topographic images of uniaxially compressed Cl adlayers on Cu(111). The compression direction is indicated with gray arrows. Part (a) shows the atomic resolution of the Cl adlayer, imaged at +1.0 V. The striped pattern allows us to differentiate between Cl atoms adsorbed in hollow sites and those in bridge sites. The Cl – Cl row spacing is shorter between adjacent hollow and bridge rows (indicated by yellow arrows) than between adjacent hollow rows (indicated by cyan arrows), leading to reduced contrast between the atomic rows. Part (b) shows the enlarged area indicated by the red square in (a). Here, atoms in bridge sites can be distinguished by following the atomic rows along the compressed axes. A small offset is present at bridge sites. The black lines help to track this offset. The black, pink, and green circles represent Cl atoms occupying fcc, hcp, and bridge sites, respectively. These were assigned by analyzing the image in panel (c), where high current was applied to desorb some of the Cl atoms, forming a large $(\sqrt{3} \times \sqrt{3})R30^\circ$ domain. Since in the uncompressed $(\sqrt{3} \times \sqrt{3})R30^\circ$ structure the Cl atoms all occupy fcc sites, we assign the Cl atoms in the largest domain to fcc sites.

be temporarily displaced, allowing an excess of chloroform to react with the surface. It is well established that, at room temperature, chloroform initially physisorbs on Cu(111) before the C–Cl bonds break sequentially, leaving three Cl atoms and a C–H radical adsorbed on the surface. The C–H radical diffuses on the surface until it meets another, and it reacts to form ethyne, which then desorbs [9].

Figures 2(a) and 2(b) show the $(19 \times \sqrt{3})$ structure, corresponding to a coverage of 7/19 ML. Here domains alternate between two and three atomic rows wide and are separated by rows of Cl atoms adsorbed in bridge sites. The atoms in bridge sites can be distinguished from those in hollow sites by analyzing the topography. Since the inter-row distance is shorter between a row of Cl atoms in hollow sites and a row of Cl atoms in bridge sites than between two rows of atoms in hollow sites, the contrast between the atoms is reduced. Therefore, where there is greater contrast between two atomic rows, indicated by the cyan arrow in Fig. 2(a), atoms in these rows can be assigned to hollow sites. Where there is reduced contrast between an atomic row and the row on either side of it, indicated by yellow arrows, the atoms in this row can be assigned to bridge sites. Alternatively, the bridge sites can be identified by noticing that atomic rows in adjacent domains do not align exactly. The atomic row (along the uncompressed direction) where there is an offset between adjacent rows in both of the other two (compressed) directions, as indicated by the black lines in Fig. 2(b), can be identified as the bridge site.

However, due to the symmetry of the structure, the fcc domains cannot be differentiated from the hcp domains by analysis of the topography alone. To identify the adsorption site, this adlayer was modified by locally applying a large cur-

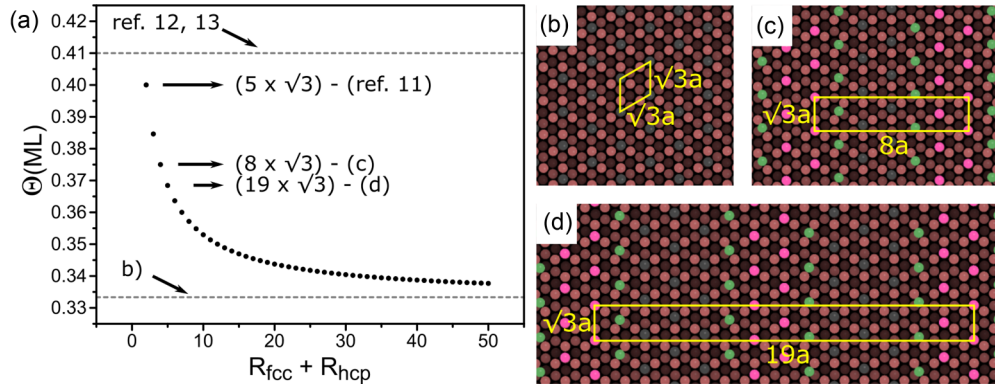


FIG. 3. Coverage vs structure relationship in the uniaxial compression regime. R_{fcc} and R_{hcp} represent the number of atomic rows in the fcc and hcp domains, respectively. Black, pink, and green spheres represent Cl atoms occupying fcc, hcp, and bridge sites, respectively. Part (a) shows the coverage decaying exponentially to $1/3$ ML (indicated by the lower dashed line), corresponding to the $(\sqrt{3} \times \sqrt{3})R30^\circ$ structure [presented in (b)], as the domain widths increase. The upper dashed line in (a) corresponds to the maximum coverage structure in the uniaxial compression regime. Part (c) shows the $(8 \times \sqrt{3})$ structure where domains, two atomic rows wide, of Cl atoms occupying fcc sites are separated from hcp domains by a row of Cl atoms in bridge sites. Part (d) shows a model of the $(19 \times \sqrt{3})$ structure, shown in Fig. 2(a), where the fcc and hcp domains are both three and two atomic rows wide, respectively.

rent and desorbing some of the Cl atoms to form large domains [see the left side of Fig. 2(c)]. Since it was previously established that Cl atoms occupy fcc sites in the $(\sqrt{3} \times \sqrt{3})R30^\circ$ adlayer [3], due to the slightly larger adsorption energy relative to the hcp sites [15], the large domain is assumed to consist of Cl atoms occupying fcc sites.

The relationship between Cl coverage and structure in the uniaxial compression regime is described in Fig. 3. At $1/3$ ML the chlorine atoms occupy the Cu(111) fcc sites in the isotropic $(\sqrt{3} \times \sqrt{3})R30^\circ$ structure [1,16], which is marked by the lower dashed line in Fig. 3(a) and shown schematically in Fig. 3(b). As the coverage increases, crowding interstitials appear on the surface, which then condense into domain walls resulting in a nonuniform uniaxial compression of the $(\sqrt{3} \times \sqrt{3})R30^\circ$ structure [11]. The domains get progressively smaller as the coverage increases. The $(8 \times \sqrt{3})$ structure shown in Fig. 2(a) is indicated in Fig. 3(a), and shown schematically in Fig. 3(c). The $(19 \times \sqrt{3})$ structure, shown schematically in Fig. 3(d), was also observed after electrospraying chloroform on clean Cu(111). The $(5 \times \sqrt{3})$ structure, indicated in Fig. 3(a), corresponding to alternating fcc and hcp domains one atomic row in width, has been previously reported for Cl on Ag(111) [11]. Between $3/8$ and $9/17$ ML, where Cl atoms occupy fcc, hcp, and bridge sites only, the relationship between coverage in monolayers Θ , the number of chlorine atoms per unit cell N_A , and the length of the unit cell L are given by

$$\Theta = \frac{N_A}{2L}, \quad (1)$$

where N_A is related to the number of atomic rows in the fcc domain R_{fcc} and the number of atomic rows in the hcp domain R_{hcp} according to the following equation:

$$N_A = (b + 1)(R_{fcc} + R_{hcp} + 2), \quad (2)$$

and the unit-cell length is

$$L = \frac{b + 1}{2}(3R_{fcc} + 3R_{hcp} + 4), \quad (3)$$

where $b = (R_{fcc} + R_{hcp}) \% 2$.

The most compressed structure possible under the uniaxial compression regime is the $(12 \times \sqrt{3})$ structure [12,13], corresponding to a coverage of $5/12$ ML [indicated by the upper dashed line in Fig. 3(a)]. At coverages between 0.4 and $5/12$ ML, single-row fcc and hcp domains are separated by domain walls several rows wide, where the chlorine atoms occupy adsorption sites that are less symmetric than bridge sites.

Scanning tunneling spectroscopy (STS) data are presented in Fig. 4. The differential conductance, measured between ± 1.0 and ± 3.0 V using constant-current spectroscopy [also known as $Z(V)$ spectroscopy], is plotted in Fig. 4(a). Constant-current spectroscopy involves measuring the dI/dV signal as the tip-sample separation increases in response to increasing sample bias voltage. This approach is useful for measuring a wide bias range where loss of signal would be expected for constant height spectra. However, constant-current spectroscopy is not suitable for measurements close to the Fermi level, since at low biases this leads to very small tip-sample distances, and therefore extreme tip-sample forces, which can modify the tip and/or sample. Variable-height spectroscopy was used to access the low bias range between ± 1.0 V. Here the bias is swept and the tip-sample distance varies in a predetermined way that maximizes the signal-to-noise ratio of the measured current and dI/dV signals. These data were used to extract the combined tip-sample LDOS $\rho_{s,t}(V)$. Variable-height spectroscopy, and the approach used to extract the LDOS from the resulting data, were described by Naydenov *et al.* [17].

We observe a peak at $+1.8$ V in the empty states. This peak is blueshifted by approximately 200 mV when measured on a hcp domain compared to a fcc domain. Since the Cl p_x and p_y orbitals are doubly occupied, and therefore below the Fermi energy, we assign the observed STS peak to an interface state between the Cu d orbitals and the Cl $3 p_z$ state. While there are no significant antibonding features in the partial density of states (PDOS) spectrum calculated by Peljhan and Kokalj [8], the calculated spectrum only extends 2 eV into the empty states. Considering that calculated energy

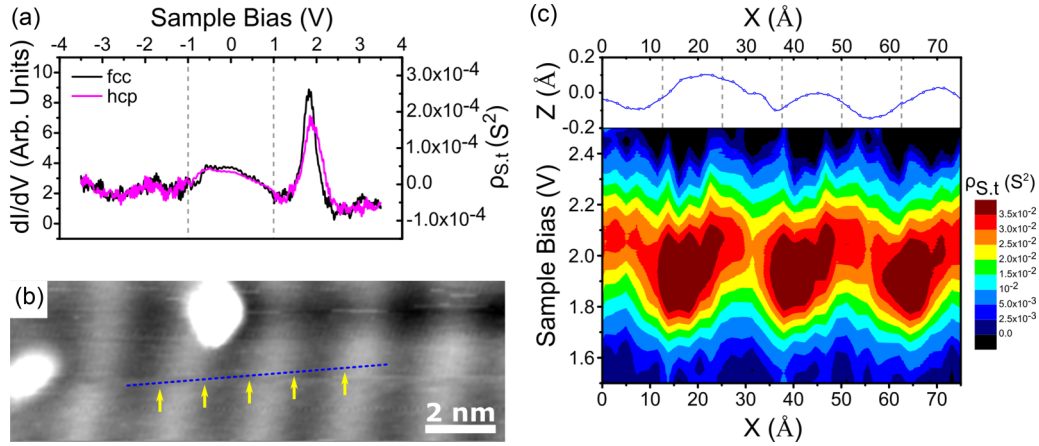


FIG. 4. STS of the $(8 \times \sqrt{3})$ Cl overlayer. Part (a) shows the STS of fcc (black) and hcp (pink) Cl domains. From ± 1.0 to ± 3.0 V, the differential conductance was measured using $Z(V)$ spectroscopy. Between -1.0 and $+1.0$ V, the LDOS, extracted from variable-height spectra, is shown. The peak at $+1.8$ V is attributed to the interaction of the Cl $3 p_z$ state with the Cu d states. This state is blueshifted by approximately 200 mV on the hcp site relative to the fcc site. A topographic STM image at $+2.0$ V, where the fcc domains appear as ridges and the hcp domains appear as valleys, is shown in (b). The energetic shift in the observed state between the fcc and hcp domains is shown more clearly in the LDOS contour map in (c). Variable-height spectra were measured along the blue dotted line in (b), and from each the LDOS was extracted [17]. The maxima can be seen to follow the domain type. Approximate positions of the Cl bridging rows are indicated by the yellow arrows in (b) and the dashed lines in (c).

scales often need adjusting to match experimental results, and that the antibonding Cu d -Cl $3 p_z$ interaction is expected to be strong, this state may simply lie outside the calculated range. Since the Cu s, d -Cl $3 p_{x,y}$ bonding interaction, and the Cu d -Cl $3 p_{x,y}$ antibonding interaction are accounted for in the calculated PDOS, we anticipate the antibonding interaction between the Cu d and Cl $3 p_z$ states to be the next state available in the wider energy range for tunneling in these measurements. There are no other features in the tunneling window between $+3.5$ and -3.5 V. It is unclear why no corresponding state is observed for the Cl atoms occupying bridge sites, despite the difference in Cl adsorption energy between hollow and bridge sites being only ~ 80 – 90 meV [10].

The shift of the observed state is shown in more detail in Fig. 4(c), where the combined tip-sample LDOS has been extracted, as described above, from variable-height spectra measured across several domains [blue dashed line in Fig. 4(b)]. There was a small lateral drift during the acquisition of the spectra, which appears as an offset in the angle of the line across which the spectra were measured, so that these data were not precisely recorded perpendicular to the long axis of the domains. The topography of the $(8 \times \sqrt{3})$ structure [shown schematically in Fig. 3(c)] at $+2.0$ V is presented in Fig. 4(b). At this bias, we lose atomic resolution and the fcc domains appear as ridges in the topography. Similar features have been observed in the topography of Cl adlayers on Ag(111), where the dark features they observe in the topography at $+1.98$ V were attributed to areas of increased chlorine density, i.e., centered around the bridging rows [11]. The approximate positions of the bridging rows are indicated by the yellow arrows in Fig. 4(b) [and the dashed lines in the topographic profile in Fig. 4(c)]. If the topographic feature were due to the increased density of Cl atoms around the domain walls, it should be centered on, and have the same periodicity as, the yellow arrows. Since this is not the case, we instead attribute

the bright features to fcc domains and the dark features to hcp sites. (See Fig. S1 in the Supplemental Material for more details [18].) The maxima in the LDOS contour map in Fig. 4(c) can be seen to shift from approximately $+1.9$ V on the fcc domains to approximately $+2.1$ V on the hcp domains.

To investigate the origin of this shift, two Gaussians were fitted to each spectrum. The widths of the Gaussians were set to be equal within each fit. The average width across all the spectra was obtained and the peaks were refit with the widths fixed at the average value of 0.4 V, and the centers free to vary. The average value of the two peak centers was 1.91(7) and 2.14(6) V, respectively. Each spectrum was refit with the peak centers fixed at these values. Samples of the fits are shown in Fig. 5(a). The amplitudes of the two peaks for the spectra in Fig. 4(c) are shown in Fig. 5(b). The peak heights are antiphase to each other, and follow the topography, with the peak at $+1.91$ V being strongest on the fcc domains and the peak at $+2.14$ V being strongest on the hcp sites. The observed shift is therefore due to the variation in the amplitude of the relative local contribution from the fcc-Cl and hcp-Cl peaks, rather than a shift in the energy of either of these peaks. Since the amplitude of the fcc peak is nonzero in the hcp domains, and *vice versa*, it is clear that these states are not strongly localized. We postulate that the energy difference between the fcc state and the hcp state is due to the change in magnitude of the dipole between the two sites. No difference in the measured apparent barrier height could be resolved between the two domains, possibly due to the fact that the expected difference is similar to the margin of error of the measurement. However, DFT calculations show that the charge on a Cl atom occupying a hcp site is higher than on one in a fcc site [8] due to the increased number of immediate Cu neighbors, and that the work function is expected to be 0.04 eV higher for a hcp domain than for a fcc domain [19]. Indeed, calculations of uniform Cl adlayers on Ag(111), which is closely analogous to Cu(111), show that the excess charge on the hcp Cl atom

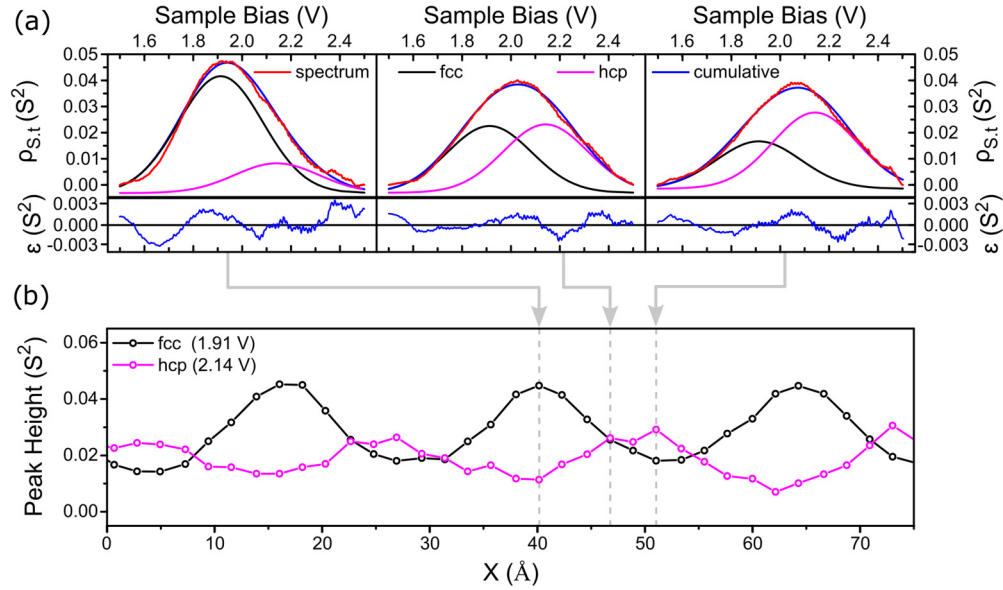


FIG. 5. Deconvolution of the LDOS measurements from Fig. 4(c) into components from the fcc and hcp sites. A linear background was subtracted from each LDOS spectrum, and two Gaussians with equal widths were fitted to each. Representative fits for spectra on the fcc, bridge, and hcp sites are shown in (a). Residuals from these fits are shown at the bottom of the panel. The variation of the peak height is shown in (b). The two peaks are antiphase and correlate with the topography. The peak at +1.91 V corresponds to the interface state between fcc Cl atoms and the Cu(111), and the peak at +2.14 V is attributed to the corresponding state for Cl atoms adsorbed in hcp sites.

resides, at least partially, in the p_z orbital [20]. The additional charge at Cl atoms adsorbed at the hcp site is likely responsible for the observed shift in the hcp unoccupied p_z state to higher energies.

Domains of various sizes were produced by applying high current as in Fig. 2. The larger domains were assumed to have fcc registry, while the domains that remained largely unchanged were assigned as hcp. This area is shown in Fig. 6(a).

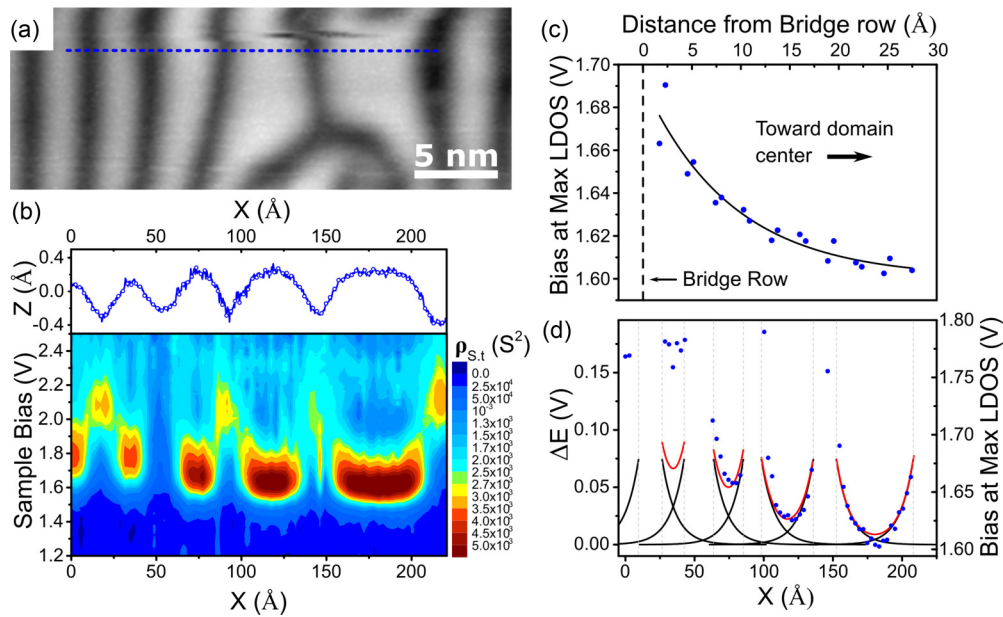


FIG. 6. STS on domains of varying size. Part (a) shows a topographic map of an area that has been modified with the tip to form domains of varying sizes. The LDOS along the blue dotted line in (a) is shown in (b). It can be seen that the energy of the state on the fcc domains shifts closer to the Fermi level as the domain gets larger. The hcp domains are the same size, and the peak position is constant at +2.1 V. To investigate the effect of the domain size, the position of the peak maximum in the largest domain was plotted as a function of the distance to the domain edge. The peak maximum was found to approach +1.6 V, which corresponds to the peak position for a uniform $(\sqrt{3} \times \sqrt{3})R30^\circ$ Cl adlayer, asymptotically as the distance from the domain edge increased. The effect of smaller domain sizes was modeled in (d) by placing the curve extracted in (c) at the locations of the bridging rows in (b). The red curves are the sums of the asymptotic curves, and the blue circles represent the measured peak positions.

The LDOS was extracted from spectra measured across these domains, along the blue dotted line in Fig. 6(a), as previously described for Fig. 4. The resulting contour map is shown in Fig. 6(b). Analysis of this plot leads to two observations:

(i) The energy of the interface state shifts closer to the Fermi level as the domain size increases.

(ii) The energy of the interface state is greater at the edge of a domain, near the bridge sites constituting the domain wall, and decays toward the center of the domain.

We now explore the latter in more detail by examining the peak behavior across the largest domain in Fig. 6(a) [between ~ 150 and 210 Å in Fig. 6(b)]. A plot of the interface state energy (approximated by the bias voltage corresponding to the maximum LDOS value) with increasing distance from the bridging row is shown in Fig. 6(c). It can be seen that, going from the domain edge toward the center, the bias value corresponding to the energy of the interface state tends asymptotically toward $+1.6$ V. We note that the interface state appears at $+1.6$ V in the STS of a uniform $(\sqrt{3} \times \sqrt{3})R30^\circ$ Cl adlayer, where every Cl atom is adsorbed in a fcc site (see Fig. S2 in the Supplemental Material). This suggests that the presence of the domain walls perturbs the interface state and shifts it to higher energies. However, it is unclear whether this is due to the increased Cl density in the vicinity of the bridge rows, or because of a specific interaction of the fcc Cl-Cu(111) interface state with the corresponding bridge Cl state (which was not detected in the available tunneling window).

The effect of domain size on the energy of the Cl-Cu(111) interface state was modeled using the relationship derived in the previous section. The approximate positions of the bridge rows, estimated from Fig. 6(b), are represented by dashed vertical lines in Fig. 6(d). The observed peak-voltage-distance relationship, fitted in Fig. 6(c), was then inserted at each of these positions. Next, the domain walls on either side were assumed to contribute additively, and the resulting predicted peak energy at every point across each fcc domain was calculated [indicated by the red curves in Fig. 6(d)]. Finally, this was compared to the measured energy of the interface state at various locations on each fcc domain, indicated by the blue circles, and it is clear that for larger domains very good agreement between the predicted and measured values is obtained. For the smallest domain, however, this simple model significantly underestimates the effect of the domain size on

the energy of the interface state, and therefore the interaction between the domain walls and the Cl-Cu(111) interface state for the smallest domains is not well described by adding the contributions from two noninteracting domain walls.

IV. CONCLUSIONS

We report STS data for uniaxially compressed Cl adlayers on Cu(111) formed by exploiting the dissociative interaction of electrosprayed chloroform with the copper surface. We observe a single peak in the empty states, which we attribute to the antibonding interaction between the Cl $3 p_z$ orbital and the Cu d states. The energy of this peak was found to be higher on the hcp domains than on the fcc domains. Decomposition of the peak into contributions from each of the adsorption sites reveals that the hcp Cl-Cu(111) interaction is approximately 230 mV more antibonding than the equivalent fcc interaction, and that the states are not well localized but leak into adjacent domains. We suggest that this energy shift is due to more charge transfer from Cu to Cl adatoms at hcp sites.

The energy of the interface state in large fcc domains was found to depend on the distance from the domain edge. The peak position was found to approach that for a pristine $(\sqrt{3} \times \sqrt{3})R30^\circ$ -Cl adlayer, where all the adatoms are in fcc sites, as the distance from the domain edge increases. The peak position was modeled for domains of different sizes based on this asymptotic-energy-distance relationship, and the predicted peak position was found to match closely the measured value, except for small domains where the peak position is underestimated. We postulate that the observed asymptotic relationship originates in the interaction between the electronic states due to Cl atoms adsorbed in bridge sites and those in fcc sites. There was no peak due to the bridging site observed in the available tunneling window. We believe these results shed important light on the ordering and interaction between Cl adatoms on Cu(111) and their influence of the local electronic structure of the surface.

ACKNOWLEDGMENT

The reported study was supported by the EU under the MolArNet project (FP7 ICT 318516) and a grant from Science Foundation Ireland (12/IA/1482).

-
- [1] P. J. Goddard and R. M. Lambert, *Surf. Sci.* **67**, 180 (1977).
 - [2] M. D. Crapper, C. E. Riley, P. J. Sweeney, C. F. McConville, D. P. Woodruff, and R. G. Jones, *Surf. Sci.* **182**, 213 (1987).
 - [3] M. D. Crapper, C. E. Riley, P. J. J. Sweeney, C. F. McConville, D. P. Woodruff, and R. G. Jones, *Europhys. Lett.* **2**, 857 (1986).
 - [4] D. P. Woodruff, D. L. Seymour, C. F. McConville, C. E. Riley, M. D. Crapper, N. P. Prince, and R. G. Jones, *Phys. Rev. Lett.* **58**, 1460 (1987).
 - [5] M. F. Kadodwala, A. A. Davis, G. Scragg, B. C. C. Cowie, M. Kerkar, D. P. Woodruff, and R. G. Jones, *Surf. Sci.* **324**, 122 (1995).
 - [6] G. Binnig, H. Rohrer, C. Gerber, and E. Weibel, *Appl. Phys. Lett.* **40**, 178 (1982).
 - [7] W. K. Walter, D. E. Manolopoulos, and R. G. Jones, *Surf. Sci.* **348**, 115 (1996).
 - [8] S. Peljhan and A. Kokalj, *J. Phys. Chem. C* **113**, 14363 (2009).
 - [9] R. G. Jones and C. A. Clifford, *Phys. Chem. Chem. Phys.* **1**, 5223 (1999).
 - [10] B. V. Andryushechkin, V. V. Zheltov, V. V. Cherkez, G. M. Zhidomirov, A. N. Klimov, B. Kierren, Y. Fagot-Revurat, D. Malterre, and K. N. Eltsov, *Surf. Sci.* **639**, 7 (2015).
 - [11] B. V. Andryushechkin, V. V. Cherkez, B. Kierren, Y. Fagot-Revurat, D. Malterre, and K. N. Eltsov, *Phys. Rev. B* **84**, 205422 (2011).
 - [12] B. Andryushechkin, K. Eltsov, and V. Shevlyuga, *Surf. Sci.* **470**, L63 (2000).

- [13] T. V. Pavlova, B. V. Andryushechkin, and G. M. Zhidomirov, *J. Phys. Chem. C* **120**, 2829 (2016).
- [14] B. Naydenov, P. Ryan, L. C. Teague, and J. J. Boland, *Phys. Rev. Lett.* **97**, 098304 (2006).
- [15] K. Doll and N. M. Harrison, *Chem. Phys. Lett.* **317**, 282 (2000).
- [16] K. Motai, T. Hashizume, H. Lu, D. Jeon, T. Sakurai, and H. W. Pickering, *Appl. Surf. Sci.* **67**, 246 (1993).
- [17] B. Naydenov and J. J. Boland, *Phys. Rev. B* **82**, 245411 (2010).
- [18] See Supplemental Material at <http://link.aps.org/supplemental/10.1103/PhysRevB.96.245411> for additional information regarding the origin of the topographic contrast at different sample voltages, and for STM/STS of the isotropic $((\sqrt{3} \times \sqrt{3})R30^\circ)$ Cl-Cu(111) surface.
- [19] H. Fu, L. Jia, W. Wang, and K. Fan, *Surf. Sci.* **584**, 187 (2005).
- [20] K. Doll and N. M. Harrison, *Phys. Rev. B* **63**, 165410 (2001).